

Comparison of the Molecular and Electronic Structures of (2,3,7,8,12,13,17,18-Octaethylporphyrinato)iron(II) and (*trans*-7,8-Dihydro-2,3,7,8,12,13,17,18-octaethylporphyrinato)iron(II)

Steven H. Strauss,^{*1a} Michael E. Silver,^{1b} Kim M. Long,^{1a} Ronald G. Thompson,^{1a} Robert A. Hudgens,^{1a} K. Spartalian,^{1c} and James A. Ibers^{1b}

Contribution from the Departments of Chemistry, Colorado State University, Fort Collins, Colorado 80523, and Northwestern University, Evanston, Illinois 60201, and Department of Physics, University of Vermont, Burlington, Vermont 05405. Received October 5, 1984

Abstract: The molecular and electronic structures of (2,3,7,8,12,13,17,18-octaethylporphyrinato)iron(II), Fe(OEP), and (*trans*-7,8-dihydro-2,3,7,8,12,13,17,18-octaethylporphyrinato)iron(II), Fe(OEC), are compared and show important differences and similarities. The compound Fe(OEP) crystallizes in space group $C_1^1-P\bar{1}$ ($Z = 1$) with unit cell dimensions $a = 4.812$ (1) Å, $b = 13.252$ (1) Å, $c = 13.369$ (1) Å, $\alpha = 113.13$ (1)°, $\beta = 92.20$ (1)°, $\gamma = 93.20$ (1)°, and $V = 781.2$ Å³. The structure has been refined to an R index on F_o^2 of 0.126 on the basis of 2022 reflections (293 K) and 187 variables. The molecule has a crystallographically imposed inversion center. The compound Fe(OEC) crystallizes in space group $D_{2h}^{14}-Pbcn$ ($Z = 4$) with unit cell dimensions $a = 21.880$ (9) Å, $b = 15.795$ (6) Å, $c = 8.554$ (4) Å and $V = 2956.2$ Å³. The structure has been refined to an R index on F_o^2 of 0.109 on the basis of 3873 reflections (123 K) and 187 variables. The molecule has a crystallographically imposed 2-fold axis passing through the unique pyrroline nitrogen atom, the iron atom, and a pyrrole nitrogen atom. The iron and four nitrogen atoms are rigorously planar in both Fe(OEP) and Fe(OEC), with iron-nitrogen bond lengths of 1.984 (5) and 2.007 (5) Å for Fe(OEP) and 1.969 (3), 1.987 (4), and 2.002 (4) Å for Fe(OEC). The last value given for Fe(OEC) is the distance from the iron atom to the pyrroline nitrogen atom. Despite the similarity in these bond distances, the porphyrin macrocycle of Fe(OEP) is essentially planar while the chlorin macrocycle of Fe(OEC) is significantly S_4 ruffled. Spectroscopic and magnetic susceptibility data demonstrate that the compounds do not have congruent electronic structures despite the fact that they both possess an intermediate-spin ($S = 1$) ground state. Solid-state effective magnetic moments (296 K) are 4.6 (1) μ_B for Fe(OEP) and 3.5 (1) μ_B for Fe(OEC). Mössbauer spectra at 4.2 K show simple quadrupole doublets for both compounds. Isomer shifts are equal to within experimental error, 0.62 (1) mm/s for Fe(OEP) and 0.63 (1) mm/s for Fe(OEC), but the quadrupole splittings are significantly different, 1.71 (1) mm/s for Fe(OEP) and 2.55 (1) mm/s for Fe(OEC). An analysis of variable-temperature ¹H NMR spectra shows that Fe(OEC) possesses rhombic magnetic anisotropy. This is the first example of resolvable ring-induced rhombicity in a metallohydrophyrin.

A variety of heme proteins and heme-containing oxidoreductase enzymes do not contain iron porphyrins but instead contain iron complexes of chlorins^{2,3} and isobacteriochlorins^{2,3} (hereafter collectively referred to as hydrophyrins). Assimilatory nitrite reductases⁴⁻⁶ and assimilatory⁷⁻¹³ and dissimilatory^{7,8} sulfite re-

ductases contain siroheme, the iron complex of the isobacteriochlorin sirohydrochlorin. The siroheme enzymes catalyze the six-electron reductions $\text{NO}_2^- \rightarrow \text{NH}_3$ and $\text{SO}_3^{2-} \rightarrow \text{H}_2\text{S}$. Dissimilatory nitrite reductases catalyze the reduction of nitrite to gaseous products (NO , N_2O , and N_2).^{14,15} and some (cytochromes cd_1) contain as the substrate binding prosthetic group an iron chlorin designated heme d_1 .¹⁶⁻²³ An iron chlorin protein that does not also contain heme c , and which exhibits nitrite reductase, hydroxylamine reductase, and catalase activities, has been isolated from *Aspergillus niger*.²⁴ Bacterial cytochromes d (cytochrome oxidase activity¹⁵) contain yet a different iron chlorin.²⁵⁻²⁸ Several

(1) (a) Colorado State University. (b) Northwestern University. (c) University of Vermont.

(2) (a) The fully unsaturated porphyrin macrocycle contains 11 conjugated double bonds. A variety of compounds are known in which the macrocyclic porphyrin skeleton is retained while one or more double bonds are removed. These compounds are formally derived from porphyrins by hydrogenation and are, therefore, commonly called hydrophyrins. Note that the generic term hydrophyrin refers to compounds in which the substituent(s) added across the double bond(s) are hydrogen atoms, alkyl or substituted alkyl groups, alkylidene groups, or oxygen or sulfur atoms: Scheer, H. In "The Porphyrins"; Dolphin, D., Ed.; Academic Press: New York, 1978; Vol. II, pp 1-44. Scheer, H.; Inhoffen, H. H. *Ibid.* pp 45-90. (b) Chlorins, which contain 10 conjugated double bonds, are porphyrins that have interrupted conjugation at vicinal C_6^3 atoms of a single pyrrole ring. The affected ring is called a pyrroline ring. Isobacteriochlorins, which contain nine conjugated double bonds, are porphyrins that contain two adjacent pyrroline rings.

(3) In the nomenclature of: Hoard, J. L. "Porphyrins and Metalloporphyrins"; Smith, K. M., Ed.; Elsevier: New York, 1975; pp 317-380.

(4) Guerrero, M. G.; Vega, J. M.; Losada, M. *Annu. Rev. Plant Physiol.* **1981**, *32*, 169-204.

(5) Jackson, R. H.; Cornish-Bowden, A.; Cole, J. A. *Biochem. J.* **1981**, *193*, 861-867.

(6) Serra, J. L.; Ibarlucea, J. M.; Arizmendi, J. M.; Llama, M. J. *Biochem. J.* **1982**, *201*, 167-170.

(7) Siegel, L. M. In "Metabolic Pathways", 3rd ed.; Greenberg, D. M., Ed.; Academic Press: New York, 1975; Vol. 7, pp 217-286.

(8) Siegel, L. M. In "Mechanisms of Oxidizing Enzymes"; Singer, T. P., Ondarza, R. N., Eds.; Elsevier-North Holland: New York, 1978; pp 201-214 and references therein.

(9) Kobayashi, K.; Yoshimoto, A. *Biochim. Biophys. Acta* **1982**, *705*, 348-356.

(10) Janick, P. A.; Rueger, D. C.; Krueger, R. J.; Barber, M. J.; Siegel, L. M. *Biochemistry* **1983**, *22*, 396-408.

(11) Janick, P. A.; Siegel, L. M. *Biochemistry* **1983**, *22*, 504-515.

(12) Christner, J. A.; Munck, E.; Janick, P. A.; Siegel, L. M. *J. Biol. Chem.* **1983**, *258*, 11147-11156.

(13) Christner, J. A.; Janick, P. A.; Siegel, L. M.; Munck, E. *J. Biol. Chem.* **1983**, *258*, 11157-11164.

(14) Losada, M. *J. Mol. Catal.* **1975-76**, *1*, 245-264.

(15) Haddock, B. A.; Jones, C. W. *Bacteriol. Rev.* **1977**, *41*, 47-99.

(16) Huynh, B. H.; Liu, M. C.; Moura, J. J. G.; Moura, I.; Ljungdahl, P. O.; Munck, E.; Payne, W. J.; Peck, H. D., Jr.; DerVartanian, D. V.; Legall, J. *J. Biol. Chem.* **1982**, *257*, 9576-9581.

(17) (a) Timkovich, R.; Cork, M. S. *Biochemistry* **1982**, *21*, 3794-3797; (b) *Ibid.* 5119-5123.

(18) Timkovich, R.; Cork, M. S.; Taylor, P. V. *J. Biol. Chem.* **1984**, *259*, 1577-1585 and references therein.

(19) Ching, Y.; Ondrias, M. R.; Rousseau, D. L.; Muhoberac, B. B.; Wharton, D. C. *Fed. Eur. Biochem. Soc., Lett.* **1982**, *138*, 239-244 and references therein.

(20) Alefounder, P. R.; Greenfield, A. J.; McCarthy, J. E. G.; Ferguson, S. J. *Biochim. Biophys. Acta* **1983**, *724*, 20-39 and references therein.

(21) Timkovich, R.; Cork, M. S. *Biochim. Biophys. Acta* **1983**, *742*, 162-168 and references therein.

(22) Kim, C. H.; Hollocher, T. C. *J. Biol. Chem.* **1983**, *258*, 4861-4863.

(23) Makinen, M. W.; Schichman, S. A.; Hill, S. C.; Gray, H. B. *Science* **1983**, *222*, 929-931 and references therein.

(24) Horie, S.; Watanabe, T.; Nakamura, S. *J. Biochem.* **1976**, *80*, 579-593.

(25) Barrett, J. *Biochem. J.* **1956**, *64*, 626-639.

(26) Newton, N. *Biochim. Biophys. Acta* **1969**, *185*, 316-331.

(27) Lemberg, R.; Barrett, J. "Cytochromes"; Academic Press: New York, 1973; pp 217-326 and references therein.

(28) Walsh, T. A.; Johnson, M. K.; Barber, D.; Thomson, A. J.; Greenwood, C. J. *Inorg. Biochem.* **1981**, *14*, 15-31.

other proteins, including *Photobacterium phosphoreum* cytochrome bd,²⁹ *Neurospora crassa* catalase,³⁰ human myeloperoxidase,³¹ sulfhemoglobin,³² and sulfmyoglobin,³³ are believed to contain iron chlorins.

The discovery of iron hdroporphyrins in these proteins has prompted chemical and spectroscopic studies of homologous³⁴ series of iron porphyrins, chlorins, and isobacteriochlorins. Conceptually, these studies have two goals, the first of which is to discover what features of the chemistry of iron hdroporphyrins differ from those of iron porphyrins. For example, it has been reported that iron-centered properties such as Fe(III)/Fe(II) potentials,³⁵⁻⁴⁰ CO and NO stretching frequencies of carbonylated³⁹ and nitrosylated⁴⁰ Fe(P)⁴¹ complexes, and CO affinities⁴² of Fe(P) are not significantly macrocycle dependent. On the other hand, we have shown that the affinity of Fe(P) for weak ligands (such as THF or ethanethiol) is strongly macrocycle dependent.⁴³ This information is necessary (although not sufficient⁴⁴) for one to learn whether a given macrocycle renders the iron atom optimally suited for a given chemical task.

The second goal is to ascertain whether, at parity of axial ligation, some metallohydrophyrins have spin states or spectroscopic parameters or both that differ from those of the corresponding metalloporphyrin. With respect to spin states of iron complexes and EPR parameters of Cu(II) complexes, no significant differences have been reported.^{35-40,45-47} EPR spectra of low- and high-spin Fe(III) complexes have been compared and show measurable but small differences.³⁵⁻⁴⁰ Surprisingly, the lack of axial symmetry of chlorin and isobacteriochlorin macrocycles itself does not afford resolvable rhombicity. Indeed, in cases where *g*-value rhombicity is observed for iron(III) porphyrins, the corresponding EPR spectra for hdroporphyrin homologues are always less rhombic or axial.

As spectra for enzymes containing iron hdroporphyrins are recorded, it is tempting to correlate the results with the only available data: spectra of iron porphyrin models. For example, Huyhn et al. concluded that reduced heme *d*₁ in *Thiobacillus denitrificans* nitrite reductase has an *S* = 2 spin state by comparing its Mössbauer spectrum to those of genuine high-spin ferrous porphyrins.¹⁶ However, since there are no published Mössbauer

spectra of appropriate iron chlorin models with known electronic structure and axial ligation,⁴⁸ it is not known whether high-spin ferrous porphyrins and chlorins have identical Mössbauer parameters. Another relevant example is the Mössbauer spectrum for reduced uncomplexed siroheme in *E. coli* sulfite reductase, which presents an apparent paradox: the isomer shift is in the range of *S* = 1 iron porphyrins while the magnitude and the temperature dependence of the quadrupole splitting are similar to *S* = 2 iron porphyrins.¹² No Mössbauer data for iron isobacteriochlorin models have been published.⁴⁸

In this paper we compare the molecular and electronic structures of Fe(OEP)⁴¹ and Fe(OEC).⁴¹ This is the first published report of structural,⁴⁹ magnetic, and Mössbauer data for an iron chlorin model compound. The comparison shows that the molecular structures of the title compounds are similar. However, Mössbauer spectra and magnetic data (μ_{eff} and variable-temperature ¹H NMR spectra) for Fe(OEP) and Fe(OEC) are strikingly different, indicating that the two compounds do not have congruent electronic structures: Fe(OEP) is axial while Fe(OEC) is rhombic. This is the first example of resolvable *ring-induced* rhombicity in a metallohydrophyrin. In addition, it is now apparent that Mössbauer parameters for similarly ligated iron porphyrins and iron hdroporphyrins can be significantly different.

Experimental Section

All manipulations and physical measurements were performed with rigorous exclusion of dioxygen and water. Benzene, hexanes, and toluene-*d*₈ (Cambridge Isotope Labs) were distilled from sodium. Dichloromethane was distilled from calcium hydride. Ethanethiol (Aldrich) was dried over 4-Å molecular sieves and then distilled under vacuum.

Lyophilized powders of Fe(OEP) and Fe(OEC) were prepared by published procedures.³⁹ These samples were used for spectroscopic and magnetic susceptibility measurements. Crystals were grown by diffusion of hexane into a solution of each compound in 9:1 (v/v) benzene/ethanethiol.⁴²

Zn(OEC) was prepared by a literature procedure.^{50,51} NMR (C_6D_6 , 22 °C) δ 1.04 (t, *J* = 7 Hz, 7,8-CH₃), 1.67 (t, *J* = 8 Hz, CH₃), 1.81 (t, *J* = 8 Hz, CH₃), 1.93 (t, *J* = 8 Hz, CH₃), 2.02 (br m, 7,8-CH_AH_B), 2.24 (br m, 7,8-CH_AH_B), 3.75 (q, *J* = 8 Hz, CH₂), 3.84 (q, *J* = 8 Hz, CH₂), 4.05 (q, *J* = 8 Hz, CH₂), 4.22 (br m, 7,8-H), 8.67 (s, 5,10-H), 9.74 (s, 15,20-H).

Crystallographic Study. Precession and Weissenberg photographs taken with Cu K α radiation indicated that Fe(OEP) crystallizes in the triclinic system; the assigned space group is $C_1^1-P\bar{1}$. Photographic work for Fe(OEC) showed systematic absences consistent with space group $D_{2h}^{12}-Pbcn$.

The crystal of Fe(OEC) was a dark-purple hexagonal rod. The crystal of Fe(OEP) was a very thin dark-purple rectangular plate. Intensity data were collected on a Picker FACS-I automatic diffractometer at -150 °C with the use of graphite-monochromated Mo K α radiation for Fe(OEC), and at 20 °C with the use of Ni-filtered Cu K α radiation for Fe(OEP). Inability to remove the exceedingly thin but only suitable crystal of Fe(OEP) from a glass capillary that was too long required removal of the low-temperature apparatus. The intensities of six standard reflections measured after every 100 reflections showed no evidence of crystal decomposition over the course of the data collection for both compounds. For Fe(OEP), 2022 unique reflections were collected and 1273 were found to have $F_o^2 > 3\sigma(F_o^2)$. For Fe(OEC), 3873 unique reflections were collected and 1929 were found to have $F_o^2 > 3\sigma(F_o^2)$. Crystal data and experimental details for both compounds are given in Table I. Both data sets were processed⁵² by using a value of 0.03 for *p* in the estimation of standard deviations.

The positions of all non-hydrogen atoms were located by use of Patterson, Fourier, and direct methods.⁵³ The final cycles of refinement were carried out on F_o^2 with the use of all 2022 reflections for Fe(OEP)

(29) Watanabe, H.; Kamita, Y.; Nakamura, T.; Takimoto, A.; Yamanaka, T. *Biochim. Biophys. Acta* **1979**, *547*, 70-78.

(30) Jacobs, G. S.; Orme-Johnson, W. H. *Biochemistry* **1979**, *18*, 2967-80.

(31) Sibbett, S. S.; Hurst, J. K. *Biochemistry* **1984**, *23*, 3007-3013.

(32) Brittain, T.; Greenwood, C.; Barber, D. *Biochim. Biophys. Acta* **1982**, *705*, 26-32 and references therein.

(33) Morell, D. B.; Chang, Y.; Clezy, P. S. *Biochim. Biophys. Acta* **1967**, *136*, 121-130 and references therein.

(34) Homologous in the sense that members of the series have the same (or very similar) peripheral substitution.

(35) Stolzenberg, A. M.; Spreer, L. O.; Holm, R. H. *J. Chem. Soc., Chem. Commun.* **1979**, 1077-1078.

(36) Richardson, P. F.; Chang, C. K.; Hanson, L. K.; Spaulding, L. D.; Fajer, J. *J. Phys. Chem.* **1979**, *83*, 3420-3424.

(37) Chang, C. K.; Fajer, J. *J. Am. Chem. Soc.* **1980**, *102*, 848-851.

(38) Chang, C. K.; Hansen, L. K.; Richardson, P. F.; Young, R.; Fajer, J. *Proc. Natl. Acad. Sci. U.S.A.* **1981**, *78*, 2652-2656.

(39) Stolzenberg, A. M.; Strauss, S. H.; Holm, R. H. *J. Am. Chem. Soc.* **1981**, *103*, 4763-4778.

(40) Fujita, E.; Fajer, J. *J. Am. Chem. Soc.* **1983**, *105*, 6743-6745.

(41) Abbreviations: OEP, 2,3,7,8,12,13,17,18-octaethylporphyrinato dianion; OEC, *trans*-7,8-dihydro-2,3,7,8,12,13,17,18-octaethylporphyrinato (octaethylchlorinato) dianion; OEIBC, 2,3,7,8-tetrahydro-2,3,7,8,12,13,17,18-octaethylporphyrinato (octaethylisobacteriochlorinato) dianion, a mixture of the *trans*,*trans*,*trans*, and *trans*,*cis*,*trans* isomers; TPP, 5,10,15,20-tetraphenylporphyrinato dianion; TMP, 5,10,15,20-tetramethylporphyrinato dianion; TMC, 7,8-dihydro-5,10,15,20-tetramethylporphyrinato dianion; TMIBC, 2,3,7,8-tetrahydro-5,10,15,20-tetramethylporphyrinato dianion; P = OEP, OEC, or OEIBC.

(42) Strauss, S. H.; Holm, R. H. *Inorg. Chem.* **1982**, *21*, 863-868 and references therein.

(43) Strauss, S. H.; Silver, M. E.; Ibers, J. A. *J. Am. Chem. Soc.* **1983**, *105*, 4108-4109.

(44) Ibers, J. A.; Holm, R. H. *Science* **1980**, *209*, 223-225.

(45) Murphy, M. J.; Siegel, L. M.; Kamin, H.; Rosenthal, D. *J. Biol. Chem.* **1973**, *248*, 2801-2814.

(46) Pelsach, J.; Blumberg, W. E.; Adler, A. *Ann. N.Y. Acad. Sci.* **1973**, *206*, 310-327.

(47) Fuhrhop, J. H.; Wasser, P. K. W.; Subramian, J.; Schroder, U. *Justus Liebig's Ann. Chem.* **1974**, 1450-1466.

(48) The results of one investigation will be submitted for publication in the near future: Strauss, S. H.; Long, K. M.; Pawlik, M. J.; Thompson, R. G.; Spartalian, K., unpublished data, 1984.

(49) A preliminary report of the molecular structure of Fe(OEC) has appeared (ref 43).

(50) Whitlock, H. W., Jr.; Hanauer, R.; Oester, M. Y.; Bower, B. K. *J. Am. Chem. Soc.* **1969**, *91*, 7485-7489.

(51) Ogoshi, H.; Watanabe, E.; Yoshida, Z.; Kincaid, J.; Nakamoto, K. *Inorg. Chem.* **1975**, *14*, 1344-1350.

(52) Corfield, P. W. R.; Doedens, R. J.; Ibers, J. A. *Inorg. Chem.* **1967**, *6*, 197-204.

(53) See Waters, J. M.; Ibers, J. A. *Inorg. Chem.* **1977**, *16*, 3273-3277 for programs and procedures.

Table I. Additional Crystallographic Details for Fe(OEP) and Fe(OEC)

compound	Fe(OEP)	Fe(OEC)
formula	C ₃₆ H ₄₆ FeN ₄	C ₃₆ H ₄₈ FeN ₄
formula weight	590.64	592.66
space group	C ₁ ¹ -P $\bar{1}$	D _{2h} ¹⁴ -Pbcn
cell dimensions		
<i>a</i> , Å	4.812 (1)	21.880 (9)
<i>b</i> , Å	13.252 (1)	15.795 (6)
<i>c</i> , Å	13.369 (1)	8.554 (4)
α, deg	113.13 (1)	90.0
β, deg	92.20 (1)	90.0
γ, deg	93.20 (1)	90.0
<i>V</i> , Å ³	781.2	2956.2
<i>Z</i>	1	4
<i>t</i> , °C	20	-150 ^a
density calcd, g/cm ³ (temp, °C)	1.255 (20)	1.331 (-150)
crystal shape	thin rectangular plate with faces of the forms {100}, {011}, and {0 $\bar{1}$ 1} with separations of 0.643, 0.108, and 0.032 mm, respectively	hexagonal rod with faces of the form {010}, {310}, {3 $\bar{1}$ 0}, {2 $\bar{1}$ 0}, and {001}
crystal volume, mm ³	0.00231	0.00530
radiation, μ (cm ⁻¹)	Cu Kα [λ(Cu Kα ₁) = 1.54056 Å], 40.91	Mo Kα [λ(Mo Kα ₁) = 0.70930 Å], 5.39
transmission factors	0.655–0.877	0.938–0.953
take-off angle, deg	3.3	3.8
receiving aperture	5.7 mm wide by 5.8 mm high; 34 cm from crystal	4.5 mm wide by 6.2 mm high; 34 cm from crystal
scan speed	2°/min	2°/min
scan width	0.8° below Kα ₁ to 1.0° above Kα ₂	0.8° below Kα ₁ to 1.2° above Kα ₂
background counts	20 s total with rescanning option ^b	20 s total with rescanning option
data collected	<i>h</i> ≥ 0, <i>k</i> ≥ 0, ± <i>l</i> ; 5.0° ≤ 2θ ≤ 120.0°	<i>h</i> ≥ 0, <i>k</i> ≥ 0, <i>l</i> ≥ 0; 3.5° ≤ 2θ ≤ 55.0°
unique data	2022	3873
unique data <i>F</i> _o ² ≥ 3σ(<i>F</i> _o ²)	1273	1929
final no. variables	187	187
error in observation of unit weight	1.66 e ²	1.36 e ²
<i>R</i> for last cycle of <i>F</i> _o ²	0.126	0.109
<i>R</i> _w for last cycle of <i>F</i> _o ²	0.155	0.144
<i>R</i> on <i>F</i> _o for data with <i>F</i> _o ² ≥ 3σ(<i>F</i> _o ²)	0.072	0.061
<i>R</i> _w on <i>F</i> _o for data with <i>F</i> _o ² ≥ 3σ(<i>F</i> _o ²)	0.074	0.060

^aThe low-temperature system is based on a design by: Huffman, J. C. Ph.D. Thesis, Indiana University, 1974. ^bThe diffractometer was run under the disk-oriented Vanderbilt system (Lenhart, P. G. *J. Appl. Crystallogr.* **1975**, *8*, 568–570).

and all 3873 reflections for Fe(OEC). Hydrogen atom positions were located in difference electron density maps; their idealized positions (C–H = 0.95 Å) were used and not varied. The isotropic thermal parameter of a hydrogen atom was assumed to be 1.0 Å² greater than that of the carbon atom to which it is attached. For Fe(OEP) the final values for *R* and *R*_w of *F*_o² are 0.126 and 0.155, respectively; the values for *R* and *R*_w on *F*_o for the reflections having *F*_o² > 3σ(*F*_o²) are 0.072 and 0.074, respectively. For Fe(OEC), the final values for *R* and *R*_w on *F*_o² are 0.109 and 0.144, respectively; the values for *R* and *R*_w on *F*_o having *F*_o² > 3σ(*F*_o²) are 0.061 and 0.060, respectively. For both Fe(OEP) and Fe(OEC) a final difference electron density map is essentially featureless.

Final positional parameters of non-hydrogen atoms and equivalent isotropic thermal parameters for Fe(OEP) and Fe(OEC) are listed in Table II. Anisotropic thermal parameters and hydrogen atom parameters (Tables III and IV), best weighted least-squares planes (Tables V and VI), and structure amplitudes (Tables VII and VIII) for Fe(OEP) and Fe(OEC), respectively, are available⁵⁴ as supplementary material. In Tables VII and VIII a negative entry for *F*_o indicates that *F*_o² < 0.

Spectroscopy. Variable-temperature ¹H NMR spectra were recorded with the following spectrometers operating at the indicated frequencies: JEOL FX-100 (99.55 MHz), Bruker SY-200 (200.13 MHz), Nicolet NT-360 (360.061 MHz). The probe temperature was measured by the method of Van Geet.⁵⁵ Because of the extreme sensitivity to dioxygen, toluene-*d*₈ solutions of Fe(OEP) and Fe(OEC) were sealed under vacuum in 5-mm NMR tubes. Chemical shifts in ppm are reported with respect to Me₄Si; a negative sign denotes an upfield shift. Mössbauer spectra were recorded with a constant acceleration spectrometer in connection with a 256-channel analyzer operating in the time-scale mode. The source was ⁵⁷Co diffused into rhodium and was kept at room temperature. Spectra were recorded in horizontal transmission geometry with an applied transverse field of 0.13 T (permanent magnet). Calibrations were made by using the hyperfine splittings in the spectrum of iron metal (line widths were typically 0.30 mm/s). Isomer shifts in mm/s are relative to iron metal at room temperature.

Magnetic Susceptibility Measurements. Solid-state magnetic susceptibilities (duplicate samples) were measured at room temperature by the

Faraday method with the use of a Cahn-Ventron 7600 magnetic susceptibility system with a Model RTL minibalace. The compound HgCo(SCN)₄ was used as the susceptibility calibrant. Lyophilized powders of Fe(OEP) and Fe(OEC) were weighed and sealed under dinitrogen in 10-mm glass sample containers. The molar diamagnetic susceptibility of the free base H₂(OEP) was found to be -470 (50) × 10⁻⁶ cm³/mol and was subtracted from the measured molar magnetic susceptibility of both Fe(OEP) and Fe(OEC) to yield molar paramagnetic susceptibilities, χ. The effective magnetic moments were calculated from the equation μ_{eff} = 2.828(χ(296))^{1/2}. The magnetic susceptibility of Fe(OEC) in toluene solution (duplicate samples) was measured by the NMR method^{56,57} and was corrected for the diamagnetism of the chlorin macrocycle as above.

Results and Discussion

Molecular Structures. In order to emphasize the differences and similarities in these two structures, Fe–N_p³ bond lengths for Fe(OEP) and Fe(OEC) are displayed in Figure 1, along with the numbering scheme used for each molecule. The structure of Fe(OEC) confirms the spectroscopic determination^{39,50,58–60} that the macrocycle is in fact a chlorin instead of the isomeric porphodimethene.⁶¹ The trans disposition of the ethyl groups on the pyrroline ring, originally deduced for the free base H₂(OEC) molecule by chemical means,⁵⁰ is also verified.

(56) Evans, D. F. *J. Chem. Soc.* **1959**, 2003–2004.

(57) Phillips, W. D.; Poe, M. In "Methods in Enzymology"; San Pietro, A., Ed.; Academic Press: New York, 1972; Vol. 24, pp 304–317.

(58) Eisner, U.; Lichtarowicz, A.; Linstead, R. P. *J. Chem. Soc.* **1957**, 733–739.

(59) Inhoffen, H. H.; Buchler, J. W.; Thomas, R. *Tetrahedron Lett.* **1969**, 1145–1148.

(60) Stolzenberg, A. M.; Spreer, L. O.; Holm, R. H. *J. Am. Chem. Soc.* **1980**, *102*, 364–370.

(61) Porphodimethenes are porphyrins with the two reducing equivalents at opposite C_m³ atoms instead of, as for chlorins, at vicinal C₃³ atoms. The structure of an iron porphodimethene has been reported: Buchler, J. W.; Lay, K. L.; Lee, Y. J.; Scheidt, W. R. *Angew. Chem. Suppl.* **1982**, 996–1003.

(54) See paragraph at the end of paper regarding supplementary material.

(55) Van Geet, A. L. *Anal. Chem.* **1970**, *42*, 679–680.

Table II. Positional Parameters for the Non-Hydrogen Atoms of Fe(OEP) and Fe(OEC)

	Fe(OEP)		
Fe	0	0	0
N(1)	0.2893 (11)	0.06095 (38)	-0.06730 (40)
N(2)	0.0801 (11)	0.13013 (40)	0.14203 (42)
C(1)	0.3688 (15)	0.01765 (53)	-0.17326 (53)
C(2)	0.5817 (15)	0.08677 (55)	-0.19101 (56)
C(3)	0.6422 (15)	0.17333 (54)	-0.09441 (58)
C(4)	0.4637 (14)	0.15650 (52)	-0.01968 (55)
C(5)	0.4479 (15)	0.22864 (50)	0.09010 (57)
C(6)	0.2671 (16)	0.21741 (53)	0.16242 (55)
C(7)	0.2512 (16)	0.29698 (53)	0.27488 (53)
C(8)	0.0619 (16)	0.25555 (52)	0.31929 (54)
C(9)	-0.0508 (16)	0.15150 (54)	0.23813 (53)
C(10)	0.2533 (16)	-0.08399 (58)	-0.25158 (53)
C(11)	0.7038 (16)	0.06938 (56)	-0.29712 (61)
C(12)	0.5429 (21)	0.11818 (74)	-0.36279 (63)
C(13)	0.8481 (16)	0.27073 (62)	-0.06937 (57)
C(14)	0.7106 (21)	0.36714 (64)	-0.07781 (75)
C(15)	0.4208 (17)	0.40599 (58)	0.32017 (53)
C(16)	0.3017 (20)	0.49077 (57)	0.28244 (66)
C(17)	-0.0294 (16)	0.30264 (51)	0.43426 (57)
C(18)	0.1167 (19)	0.25835 (63)	0.50799 (56)

	Fe(OEC)		
Fe	0	0.074796 (46)	1/4
N(1)	0.07439 (12)	0.07573 (20)	0.12050 (35)
N(2)	0	0.20057 (23)	1/4
N(3)	0	-0.05196 (23)	1/4
C(1)	0.10049 (14)	0.00788 (24)	0.04629 (42)
C(2)	0.15539 (16)	0.03258 (24)	-0.03322 (45)
C(3)	0.16322 (16)	0.11669 (24)	-0.00718 (48)
C(4)	0.11228 (15)	0.14409 (22)	0.08799 (45)
C(5)	0.10019 (16)	0.22601 (22)	0.12967 (47)
C(6)	0.04617 (15)	0.25395 (23)	0.20138 (43)
C(7)	0.02927 (16)	0.34084 (22)	0.22207 (48)
C(8)	0.02015 (15)	-0.19587 (21)	0.17848 (44)
C(9)	0.03416 (15)	-0.10274 (22)	0.15445 (47)
C(10)	0.07818 (15)	-0.07464 (25)	0.05434 (45)
C(11)	0.19700 (16)	-0.02616 (23)	-0.12182 (49)
C(12)	0.24309 (17)	-0.07187 (28)	-0.01679 (48)
C(13)	0.21491 (17)	0.17288 (24)	-0.05769 (49)
C(14)	0.26233 (17)	0.18639 (26)	0.07158 (57)
C(15)	0.06930 (17)	0.41560 (24)	0.18419 (51)
C(16)	0.11768 (19)	0.43185 (27)	0.30881 (53)
C(17)	0.07981 (20)	-0.24623 (27)	0.18762 (57)
C(18)	0.07549 (19)	-0.33837 (25)	0.22937 (65)

Bond distances and angles for both compounds are given in Table IX. For Fe(OEP) the packing consists of one molecule per triclinic unit cell with the Fe atom located on a crystallographic inversion center. The packing for Fe(OEC) consists of four identical molecules per orthorhombic unit cell, each possessing a crystallographic 2-fold axis passing through atoms N(2), Fe, and N(3). The shortest intermolecular distances between non-hydrogen atoms are 3.370 (5) Å, N(1)⋯C(9), and 3.115 (4) Å, Fe⋯C(10), for Fe(OEC), and 3.433 (9) Å, C(6)⋯C(10), and 3.465(6) Å, Fe⋯C(4), for Fe(OEP).

The iron and four nitrogens are rigorously planar in both Fe(OEP) and Fe(OEC). However, for Fe(OEC) the rest of the chlorin macrocycle is significantly S_4 ruffled (the dihedral angles (θ) between the planes of opposite pyrrole rings and the pyrrole and pyrroline ring are 23.3° and 27.4°, respectively). In contrast, the porphyrin macrocycle in Fe(OEP) is essentially planar (θ is 0.0° while the dihedral angle between the planes of adjacent pyrrole rings is 3.3°). The C_a-C_b (1.516 (5) Å) and C_b-C_b (1.508 (7) Å) distances in the pyrroline ring of Fe(OEC) are longer than the usual pyrrole values of ~1.44 and ~1.36 Å, respectively (average values 1.436 (8) and 1.334 (8) Å, respectively, for Fe(OEP)), and reflect the sp³ hybridization of the pyrroline C_b atoms. At present, Fe(TPP),^{41,62} Fe(OEP), and Fe(OEC) are the only four-coordinate Fe(II) porphyrins and hydporphyrins to be

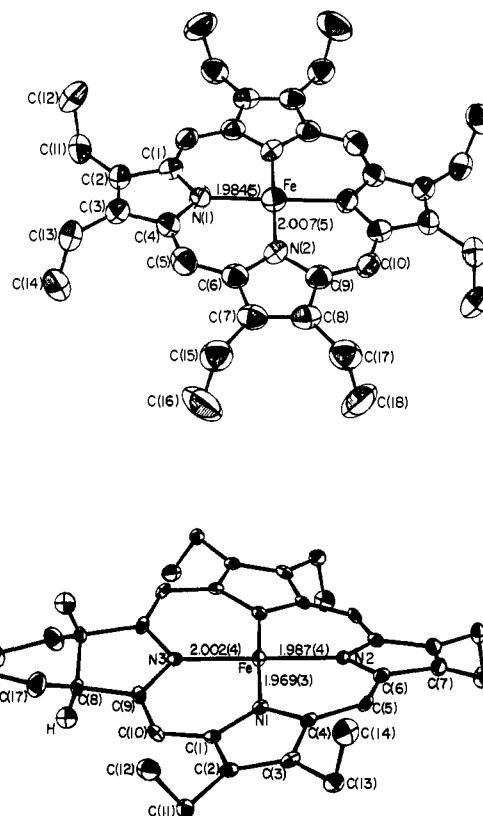


Figure 1. Drawings of the structures of Fe(OEP) (top) and Fe(OEC) (bottom) showing the labeling scheme and Fe-N_p distances (Å). Atoms not labeled are centrosymmetrically [Fe(OEP)] or 2-fold [Fe(OEC)] related. The thermal ellipsoids are drawn at the 50% probability level. H atoms, except for the two on the pyrroline C_b atoms of Fe(OEC), have been omitted for clarity.

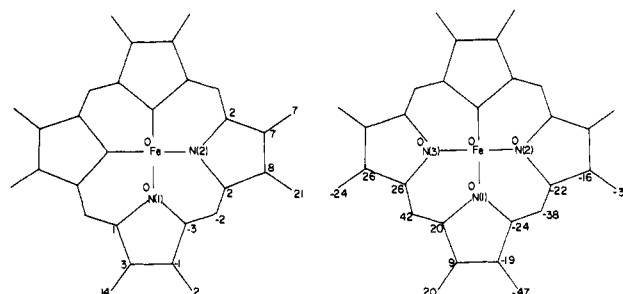


Figure 2. Deviations of the atoms (Å × 10²) from a plane containing the Fe and all four N atoms for Fe(OEP) (left) and Fe(OEC) (right). The numbering scheme is the same as in Figure 1. Methyl carbon atoms have been excluded.

structurally characterized. The compound Fe(TPP) possesses 4 site symmetry and is ruffled such that θ is 25.6°. The Fe-N_p distance in Fe(TPP), which possesses an intermediate-spin ($S = 1$) ground state in the solid state,⁶³ is 1.972 (4) Å. The range of Fe-N_p distances in Fe(OEP) and Fe(OEC) (Table IX) is in harmony with an $S = 1$ ground state for these compounds in the solid state.⁶⁴

Distances of the non-hydrogen atoms from the plane defined by the Fe and N atoms are shown in Figure 2 for Fe(OEP) and Fe(OEC). The pyrrole rings are planar, with the maximum displacement from either a least-squares plane or a plane defined by the three crystallographically unique pyrrole atoms being 0.01 and 0.06 Å for Fe(OEP) and Fe(OEC), respectively. The pyrroline ring of Fe(OEC) is less planar, with the maximum dis-

(62) Collman, J. P.; Hoard, J. L.; Kim, N.; Lang, G.; Reed, C. A. *J. Am. Chem. Soc.* **1975**, *97*, 2676-2681.

(63) Boyd, P. D. W.; Buckingham, D. A.; McMeeking, R. F.; Mitra, S. *Inorg. Chem.* **1979**, *18*, 3585-3591.

(64) Scheidt, W. R.; Reed, C. A. *Chem. Rev.* **1981**, *81*, 543-555 and references therein.

Table IX. Bond Distances and Angles in Fe(OEP) and Fe(OEC)

atoms	distance, Å		atoms	angle, deg	
	Fe(OEP)	Fe(OEC)		Fe(OEP)	Fe(OEC)
Fe-N(1)	1.984 (5)	1.969 (3)	C(9)-N(3)-C(9) ^a		108.2 (4)
Fe-N(2)	2.007 (5)	1.987 (4)	N(1)-C(1)-C(10 ['])	122.8 (6)	124.3 (3)
Fe-N(3)		2.002 (4)	N(1)-C(1)-C(2)	111.7 (6)	110.8 (3)
N(1)-C(1)	1.381 (7)	1.370 (5)	C(2)-C(1)-C(10)	125.4 (6)	124.8 (3)
N(1)-C(4)	1.386 (7)	1.389 (4)	C(1)-C(2)-C(3)	106.8 (6)	107.1 (4)
N(2)-C(6)	1.357 (8)	1.380 (4)	C(1)-C(2)-C(11)	126.2 (6)	125.3 (3)
N(2)-C(9)	1.386 (8)		C(3)-C(2)-C(11)	126.9 (7)	127.6 (3)
N(3)-C(9)		1.368 (4)	C(2)-C(3)-C(4)	106.2 (6)	106.7 (3)
C(1)-C(2)	1.424 (8)	1.434 (5)	C(2)-C(3)-C(13)	128.3 (7)	128.8 (4)
C(1)-C(10)	1.409 (8)	1.398 (5)	C(4)-C(3)-C(13)	125.5 (6)	124.4 (3)
C(2)-C(3)	1.356 (8)	1.358 (5)	N(1)-C(4)-C(3)	112.4 (6)	109.9 (3)
C(3)-C(4)	1.415 (8)	1.446 (5)	N(1)-C(4)-C(5)	121.8 (6)	124.6 (3)
C(4)-C(5)	1.410 (8)	1.368 (5)	C(3)-C(4)-C(5)	125.8 (6)	125.4 (3)
C(5)-C(6)	1.369 (9)	1.403 (5)	C(4)-C(5)-C(6)	127.0 (6)	125.1 (3)
C(6)-C(7)	1.466 (8)	1.432 (5)	C(5)-C(6)-C(7)	125.0 (7)	125.0 (3)
C(7)-C(7) ^a		1.367 (7)	N(2)-C(6)-C(5)	125.3 (6)	123.8 (3)
C(7)-C(8)	1.313 (8)		N(2)-C(6)-C(7)	109.6 (6)	111.0 (3)
C(8)-C(8) ^a		1.508 (7)	C(6)-C(7)-C(7) ^a		106.6 (2)
C(8)-C(9)	1.439 (8)	1.516 (5)	C(6)-C(7)-C(8)	107.1 (6)	
C(9)-C(10)	1.351 (9)	1.363 (5)	C(7)-C(7)-C(15) ^a		128.3 (2)
C(11)-C(2)	1.494 (9)	1.505 (5)	C(8)-C(7)-C(15)	130.5 (7)	
C(11)-C(12)	1.497 (10)	1.531 (5)	C(6)-C(7)-C(15)	122.4 (7)	125.1 (3)
C(13)-C(3)	1.501 (9)	1.501 (5)	C(8)-C(8)-C(9) ^a		103.2 (2)
C(13)-C(14)	1.512 (10)	1.531 (6)	C(7)-C(8)-C(9)	108.0 (6)	
C(15)-C(7)	1.505 (9)	1.506 (5)	C(8)-C(8)-C(17) ^a		117.2 (4)
C(15)-C(16)	1.530 (10)	1.524 (6)	C(7)-C(8)-C(17)	128.6 (6)	
C(17)-C(8)	1.507 (9)	1.531 (5)	C(9)-C(8)-C(17)	123.4 (6)	109.8 (3)
C(17)-C(18)	1.504 (10)	1.502 (6)	C(8)-C(9)-C(10)	126.1 (7)	122.9 (3)
			N(3)-C(9)-C(8)		112.2 (3)
N(1)-Fe-N(2)	90.1 (2)	89.6 (1)	N(2)-C(9)-C(8)	109.5 (6)	
N(1)-Fe-N(2) ^a	89.9 (2)		N(3)-C(9)-C(10)		124.8 (3)
N(1)-Fe-N(3)		90.4 (1)	N(2)-C(9)-C(10)	124.4 (6)	
C(1)-N(1)-C(4)	102.8 (6)	105.4 (3)	C(9)-C(10)-C(1)	127.2 (6)	125.7 (3)
C(1)-N(1)-Fe	128.4 (4)	126.8 (2)	C(2)-C(11)-C(12)	112.9 (6)	113.2 (3)
C(4)-N(1)-Fe	128.8 (4)	127.7 (2)	C(3)-C(13)-C(14)	111.6 (6)	112.6 (3)
C(6)-N(2)-C(9)	105.8 (6)		C(7)-C(15)-C(16)	112.8 (6)	112.7 (3)
C(6)-N(2)-C(6) ^a		104.7 (4)	C(8)-C(17)-C(18)	113.1 (6)	117.5 (4)
C(6)-N(2)-Fe	126.9 (5)	127.7 (2)			
C(9)-N(2)-Fe	127.2 (4)				
C(9)-N(3)-Fe		125.9 (2)			

^a Primed atoms related to unprimed atoms by $x' = -x$, $y' = -y$, $z' = -z$ for Fe(OEP) and by $x' = -x$, $y' = y$, $z' = 1/2 - z$ for Fe(OEC).

placement from the plane defined by the three crystallographically unique pyrrole atoms being 0.23 Å.

The major difference between the Fe(OEP) and Fe(OEC) structures is that the porphyrin is planar whereas the hydrophyrin is significantly S_4 ruffled. The average Fe-N_p distance is 1.996 (8) Å for Fe(OEP) and 1.986 (5) Å for Fe(OEC); therefore, the macrocycle core size may be slightly larger for Fe(OEP). For a planar conformation hydrophyrins would have intrinsically larger cores (longer distances between opposite pyrrole or pyrrole nitrogen atoms) than porphyrins, a function of the more obtuse C_a-N-C_a angle (108.2° for the pyrrole rings of Fe(OEC) as compared with average values of 105.1° and 104.3° for the pyrrole rings of Fe(OEC) and Fe(OEP), respectively) and the longer C_b-C_b distances of the pyrrole ring(s).⁶⁵⁻⁷² The S_4 distortion from planarity leads to a reduction in core size and

shorter metal-nitrogen distances relative to the planar conformation⁷³ and should be more facile for hydrophyrins owing to their decreased aromaticity. Therefore, to maintain an optimum M-N_p distance, an increase in S_4 ruffling should occur on going to the more reduced macrocycles of a homologous series. Such an increased distortion is observed on going from planar Fe(OEP) to ruffled Fe(OEC), resulting in a slightly larger core for the porphyrin. If Fe(OEP) were as ruffled as Fe(OEC), then the hydrophyrin core would be the larger.

Consideration of other related structures further demonstrates that the S_4 distortion is more readily achieved for hydrophyrins than for porphyrins when the metal has optimum M-N_p distances less than 1.99 Å, as do low- and intermediate-spin Fe(II)⁶⁴ and Ni(II).^{71,73-75} The tetragonal form of Ni(OEP)⁷⁵ and Ni(OEiBC)⁷¹ have average Ni-N_p distances of 1.93 Å. However, in the porphyrin θ is 28° while in the isobacteriochlorin it averages 48°. Here the isobacteriochlorin must undergo a considerably larger S_4 distortion to achieve the same Ni-N_p distance because of the intrinsically larger core.⁷⁶ Similarly, structures of the TMP⁴¹, TMC⁴¹, and TMI⁴¹ complexes of Ni(II)⁶⁸⁻⁷⁰ reveal the porphyrin to be essentially planar while the chlorin and iso-

(65) Hoppe, W.; Will, G.; Gassmann, J.; Weichselgartner, H. Z. *Kristallogr.* **1969**, *128*, 18-35.

(66) Spaulding, L. D.; Andrews, L. C.; Williams, G. J. B. *J. Am. Chem. Soc.* **1977**, *99*, 6918-6923.

(67) (a) Barkigia, K. M.; Fajer, J.; Spaulding, L. D.; Williams, G. J. B. *J. Am. Chem. Soc.* **1981**, *103*, 176-181. (b) Barkigia, K. M.; Fajer, J.; Chang, C. K.; Williams, G. J. B. *J. Am. Chem. Soc.* **1982**, *104*, 315-317.

(68) Ulman, A.; Gallucci, J.; Fisher, D.; Ibers, J. A. *J. Am. Chem. Soc.* **1980**, *102*, 6852-6854.

(69) Gallucci, J. C.; Swepston, P. N.; Ibers, J. A. *Acta Crystallogr., Sect. B* **1982**, *38*, 2134-2139.

(70) Suh, M. P.; Swepston, P. N.; Ibers, J. A. *J. Am. Chem. Soc.* **1984**, *106*, 5164-5171.

(71) Kratky, C.; Angst, C.; Johansen, J. E. *Angew. Chem., Int. Ed. Engl.* **1981**, *20*, 211-212.

(72) Cruse, W. B. T.; Harrison, P. K.; Kennard, O. *J. Am. Chem. Soc.* **1982**, *104*, 2376-2380.

(73) J. L. Hoard, *Ann. N.Y. Acad. Sci.* **1973**, *206*, 18-31.

(74) Meyer, E. F. *Acta Crystallogr., Sect. B* **1972**, *28*, 2162-2167.

(75) Cullen, D. L.; Meyer, E. F., Jr. *J. Am. Chem. Soc.* **1974**, *96*, 2095-2102.

(76) The structure of one nickel(II) hexahydrophyrin (three adjacent reduced pyrrole rings) is severely distorted toward S_4 symmetry with nearly coplanar nickel and nitrogen atoms. However, no bond distances or angles were reported: Johansen, J. E.; Piermattie, V.; Angst, C.; Diener, E.; Kratky, C.; Eschenmoser, A. *Angew. Chem., Int. Ed. Engl.* **1981**, *20*, 261-263.

Table X. Molecular and Electronic Structural Data for $d^6 S = 1$ Compounds

compd	M-N, Å	magnetic data ^a			Mössbauer data ^a		
		$\mu_{\text{eff}}(\mu_{\text{B}})$	temp range, K	D, cm^{-1b}	temp, K	$\delta, \text{mm/s}$	$\Delta E_{\text{Q}}, \text{mm/s}$
Fe(OEC) ^d	1.969 (3)	3.5	296		4.2	0.63	2.55
	1.987 (4)						
	2.002 (4)						
Fe(OEP) ^d	1.984 (5)	4.6	296		4.2	0.62	1.71
	2.007 (5)						
Fe(TPP) ^e	1.972 (4)	4.2	100–296	90	4.2	0.52	1.51
					296	0.42	1.52
Fe(Pc) ^f	1.927 (1)	3.7–3.9	105–296	64	78	0.33	1.97
	1.926 (1)				300	0.26	2.02
Fe(C ₂₂ H ₂₂ N ₄) ^g	1.915 (3)	3.69	77–296				
	1.916 (3)						
	1.917 (3)						
	1.922 (3)						
Fe(octaaza[14]annulene) ^h	1.846 (4)	2.9–3.0	40–296		77	0.19	4.13
	1.826 (4)				300	0.11	4.04
Fe([15]aneN ₄)NO ₂ ⁺ ⁱ		3.36	100–350		298	0.33	≤0.4
Fe(phen) ₂ Ox·5H ₂ O ^j		3.7–3.8	10–296	~3	4.2	0.24	0.28
					298	0.23	0.31
Fe(phen) ₂ F ₂ ·4H ₂ O ^j		5.2	10–296	~3	4.2	0.25	0.30
Co(3-Pr-biuret) ₂ ^{-k}	1.88 (2)	3.0–3.1	100–296	54	298	0.24	0.32

^aSolid-state measurements. ^bZero field splitting. ^cIsomer shift relative to iron metal. ^dThis work. Literature values for Fe(OEP)⁸¹ (temperature): $\mu_{\text{eff}} 4.7 \mu_{\text{B}}$ (296 K); $\delta 0.59 \text{ mm/s}$, $\Delta E_{\text{Q}} 1.60 \text{ mm/s}$ (4.2 K). ^eReferences 62 (structure = str), 63 (magnetic data = mag), and 80 (Mössbauer data = Moss). ^fPc = phthalocyanine; ref 77 (str), 78 (mag), and 79 (Moss). ^gC₂₂H₂₂N₄ = 7,16-dihydro-6,8,15,17-tetramethyldibenzo[*b,i*]-[1,4,8,11]tetraazacyclotetradecinato(2-); all data from ref 82. ^hReferences 83 (str) and 84 (mag and Möss). ⁱAll data from ref 85. ^jAll data from ref 86. ^kReferences 87 (str) and 88 (mag and Möss).

bacteriochlorin, with θ ranging from 35° to 38° and from 42° to 45°, respectively, display increasing distortion.

Note that a comparison of the structures of Fe(OEP) and the triclinic form of Ni(OEP)⁷⁵ shows that the S_4 distortion is not the only degree of freedom by which M-N_p bonds can be shortened. Both compounds are planar with $\theta = 0^\circ$, yet the average Fe-N_p distance is 1.996 (8) Å and the average Ni-N_p distance is 1.958 (1) Å.

To summarize, two points can be made. Given that all structurally characterized Ni(II) and Fe(II) hydroporphyrins are distorted while both planar and distorted porphyrins are known, (i) hydroporphyrins distort more easily than porphyrins and (ii) the energy barrier for contraction of the macrocycle core (with resulting nonplanarity) upon complexation to small metals such as Ni(II) and low- or intermediate-spin Fe(II) is small, as previously noted by Hoard.⁷³ The greater structural compliance of hydroporphyrins over porphyrins may be a factor of chemical,⁴³ and therefore biological, significance.

Electronic Structures. (a) **Magnetic Moments and Mössbauer Spectra.** A variety of d^6 complexes of Fe(II) and Co(III) with intermediate-spin state $S = 1$ have been studied.^{77–90} Structural,

magnetic, and Mössbauer data for these compounds are collected in Table X. This fascinating electron configuration, which exhibits unusually wide ranges of effective magnetic moments, zero field splittings, and Mössbauer quadrupole splittings, has been the focus of several ligand field^{63,91–93} and ab initio calculations.^{94,95}

Despite the similarity of the Fe(OEC) and Fe(OEP) molecular structures, especially the Fe-N_p bond distances, the room temperature magnetic moments of these two compounds are markedly different (Table X). These solid-state moments, 3.5 (1) μ_{B} for Fe(OEC) and 4.6 (1) μ_{B} for Fe(OEP), are well within the range of values observed for intermediate-spin ($S = 1$) compounds of Fe(II) and Co(III). Our measured value for Fe(OEP) agrees with the value reported earlier by Dolphin and co-workers (4.7 (1) μ_{B}).⁸¹ To demonstrate that the difference in μ_{eff} for Fe(OEC) and Fe(OEP) is not the result of a solid-state effect, we have measured the magnetic moment for Fe(OEC) in solution by the NMR method (see Experimental Section): $\mu_{\text{eff}} = 3.4$ (1) μ_{B} in toluene at 296 K. An accurate measurement of μ_{eff} for Fe(OEP) in solution has been hampered by the low solubility ($\sim 0.6 \text{ mM}$) of this compound in toluene. The magnetic measurements indicate that Fe(OEC) and Fe(OEP) both possess $S = 1$ spin states, in harmony with the molecular structures described above. While we have not yet obtained variable-temperature susceptibility data for these compounds, variable-temperature ¹H NMR spectra (see below) clearly show that for both compounds the $S = 1$ ground state is not in thermal equilibrium with other spin states over the temperature range 183–348 K. Despite these similarities, the large difference in μ_{eff} indicates that Fe(OEC) and Fe(OEP) do not have congruent electronic structures.

Mössbauer spectra at 4.2 K are another indication that the two compounds are different electronically (Table X). The isomer shifts are equal within experimental error, which can be interpreted as indicating that the Fe 4s electron density and the shielding provided by the six d electrons are equally balanced for Fe(OEC) and Fe(OEP).⁹⁶ However, the large difference in quadrupole

(77) Kirner, J. F.; Dow, W.; Scheidt, W. R. *Inorg. Chem.* **1976**, *15*, 1685–1690.

(78) Barraclough, C. G.; Martin, R. L.; Mitra, S.; Sherwood, R. C. *J. Chem. Phys.* **1970**, *53*, 1643–1648.

(79) Dale, B. W.; Williams, R. J. P.; Edwards, R. J.; Johnson, C. E. *J. Chem. Phys.* **1968**, *49*, 3445–3449.

(80) Lang, G.; Spatalian, K.; Reed, C. A.; Collman, J. P. *J. Chem. Phys.* **1978**, *69*, 5424–5427.

(81) Dolphin, D.; Sams, J. R.; Tsin, T. B.; Wong, K. L. *J. Am. Chem. Soc.* **1976**, *98*, 6970–6975.

(82) Goedken, V. L.; Pluth, J. J.; Peng, S.-M.; Bursten, B. *J. Am. Chem. Soc.* **1976**, *98*, 8014–8021.

(83) Little, R.; Ibers, J. A.; Baldwin, J. E. *J. Am. Chem. Soc.* **1975**, *97*, 7049–7053.

(84) Reiff, W. M.; Wong, H.; Baldwin, J. E.; Huff, J. *Inorg. Chim. Acta* **1977**, *25*, 91–96.

(85) Watkins, D. D.; Riley, D. P.; Stone, J. A.; Busch, D. H. *Inorg. Chem.* **1976**, *15*, 387–393.

(86) König, E.; Ritter, G.; Kanellakopulos, B. *J. Chem. Phys.* **1973**, *58*, 3001–3009.

(87) Bour, J. J.; Beurskens, P. T.; Steggarda, J. J. *J. Chem. Soc., Chem. Commun.* **1972**, 221–222.

(88) König, E.; Schnakig, R.; Kanellakopulos, B. *J. Chem. Phys.* **1975**, *62*, 3907–3911.

(89) König, E.; Madeja, K. *Inorg. Chem.* **1968**, *7*, 1848–1855.

(90) Birker, P. J. M. W. L.; Bour, J. J.; Steggarda, J. J. *Inorg. Chem.* **1973**, *12*, 1254–1259.

(91) König, E.; Schnakig, R. *Theor. Chim. Acta* **1973**, *30*, 205–208.

(92) König, E.; Schnakig, R. *Inorg. Chim. Acta* **1973**, *7*, 383–392.

(93) Mispelter, M.; Momenteau, M.; Lhoste, J. M. *J. Chem. Phys.* **1980**, *72*, 1003–1012.

(94) Obara, S.; Kashigawa, H. *J. Chem. Phys.* **1982**, *77*, 3115–3165.

(95) Dedieu, A.; Rohme, M.-M.; Veillard, A. *Adv. Quantum Chem.* **1982**, *16*, 43–95.

(96) Sams, J. R.; Tsin, T. B. In "The Porphyrins"; Dolphin, D., Ed.; Academic Press: New York, 1979; Vol. 4, pp 425–478.

Table XI. Linear Least-Squares Parameters for δ vs. $1/T$ Plots^a

compd	resonance	10^{-3} slope, ppm·K	$\delta,^b$ ppm	$\delta,^c$ ppm
Fe(OEP)	meso	19.0	10.6	10.1
	CH ₂	8.5	4.0	4.1
	CH ₃	3.4	1.5	1.9
Fe(OEC)	a meso	16.3	15.0	9.7 or 8.7
	b meso	15.8	12.0	9.7 or 8.7
	c CH ₂	21.0	-8.5	4.0 or 3.8
	d CH ₂	16.4	-8.1	4.0 or 3.8
	e CH ₃	11.2	-10.9	1.9, 1.8, or 1.7
	f β -H	-12.2	65.6	4.2
	g CH ₂	-8.7	33.9	4.0 or 3.8
	h CH ₃	-5.6	15.3	1.9, 1.8, 1.7, or 1.0
	i CH ₃	-8.5	15.3	1.9, 1.8, 1.7, or 1.0
	j CH _A H _B	-13.2	27.9	2.2 or 2.0
	k CH _A H _B	-19.9	44.9	2.2 or 2.0

^a Figures 3 and 5. ^b δ at $1/T = 0$, extrapolated. ^c δ for diamagnetic reference. For Fe(OEP) the diamagnetic reference compound is Ni(OEP) (see ref 97); for Fe(OEC) the reference is Zn(OEC) (see Experimental Section).

splitting is probably due in part to differences in the way that the six d electrons are distributed in the four closely spaced d orbitals (i.e., xy , xz , yz , z^2).^{80,94-96} Mössbauer spectra in a strong applied field at various temperatures are in progress. These are expected to allow us to determine the sign of the electric field gradient, the sign of the asymmetry parameter, η , and the induced magnetic hyperfine field. These spectra will greatly aid in elucidating the detailed electronic differences between Fe(OEC) and Fe(OEP). For this reason we hesitate to interpret the present data any further. Nevertheless, we can conclude from this one example that Mössbauer parameters for similarly ligated iron porphyrins and iron hydroporphyrins *can* be significantly different.

(b) **Variable-Temperature ¹H NMR Spectra.** During our investigation of the non-Curie behavior of Fe(OEC) (see below), we studied the temperature dependence of the ¹H NMR spectrum of Fe(OEP) dissolved in toluene-*d*₈. Spectra obtained at room temperature for Fe(OEP) dissolved in benzene-*d*₆^{97,98} and variable-temperature spectra for this compound in dichloromethane-*d*₂⁹⁸ have been reported. Large isotropic shifts with significant dipolar contributions and narrow line widths are characteristic of Fe(OEP) and all other four-coordinate iron(II) porphyrins studied to date.^{93,97-101} Our data are summarized in Table XI and displayed in Figure 3.¹⁰² The strict adherence to Curie behavior¹⁰³ demonstrates that the $S = 1$ ground state of Fe(OEP) is not in thermal equilibrium with other spin states over the accessible temperature range (-90 to 75 °C). Our data sharply contrast the reported curvature in plots of δ vs. $1/T$ for Fe(OEP) in dichloromethane-*d*₂.⁹⁸ However, Fe(OEP) reacts with dichloromethane to produce Fe(III) species, including FeCl(OEP),⁴² the half-life of Fe(OEP) in neat dichloromethane at 25 °C is ~ 3 h.¹⁰⁴ Thus, the use of CH₂Cl₂ as a solvent for Fe(P) complexes may lead to a mixture of Fe(II) and Fe(III) complexes and is not desirable.

The 100-MHz ¹H NMR spectrum of Fe(OEC) dissolved in toluene-*d*₈ at 6 °C is shown in Figure 4. Each resonance is lettered (a-k) to facilitate the discussion below; the assignment of the

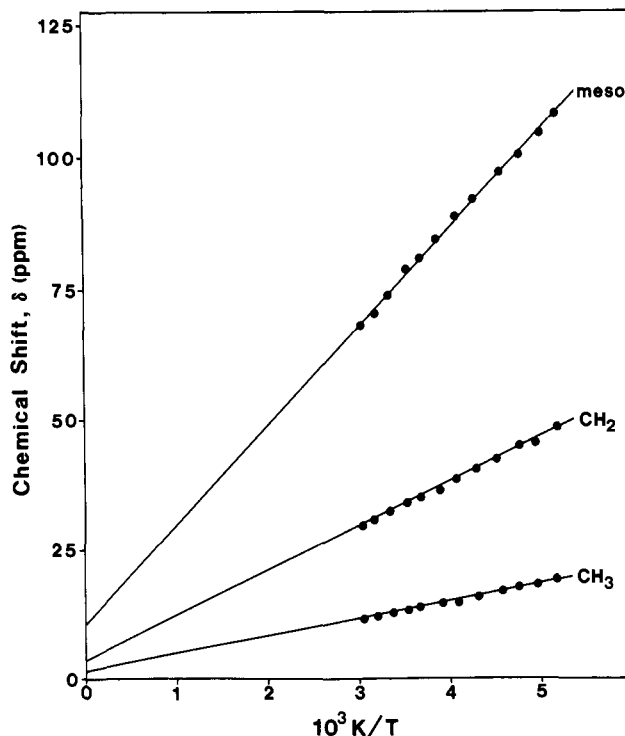


Figure 3. δ vs. $1/T$ plots for 200-MHz ¹H NMR spectra of Fe(OEP) in toluene-*d*₈. The solid lines are linear least-squares fits to the data and are extrapolated to $1/T = 0$.

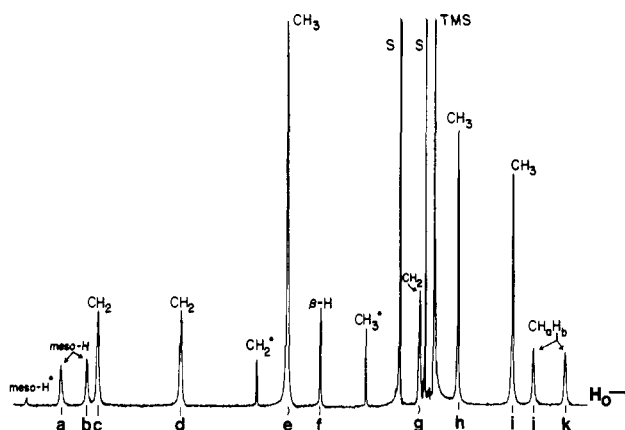


Figure 4. 100-MHz ¹H NMR spectrum of Fe(OEC) in toluene-*d*₈ at 6 °C. Signal assignments are indicated (S = solvent). The resonances marked with asterisks are due to Fe(OEP).

spectrum follows an earlier study³⁹ and is in harmony with the integrated ratios of the resonances and C₂ molecular symmetry. Especially noteworthy is that two sets of methyl protons are accidentally isochronous *at all temperatures* and give rise to resonance e. The C₂ symmetry of Fe(OEC) dictates that all four sets of methylene protons are diastereotopic. Among the methylene protons for the diamagnetic C₂ compounds H₂(OEC) and Zn(OEC), the pyrroline CH_AH_B protons exhibit the largest chemical shift difference,¹⁰⁵ so it is reasonable to assign resonances j and k to these protons in the spectrum of Fe(OEC).

The temperature dependence of the Fe(OEC) spectrum is shown in Figure 5 and summarized in Table XI.^{102,103} Some chemical shifts could not be determined accurately over the entire temperature range employed. In some cases resonances were masked by solvent or Me₄Si (e.g., resonances f and g) or by other resonances (e.g., resonance c masks resonance a at low temperatures). In addition, all resonances broadened appreciably at low tem-

(97) Goff, H.; La Mar, G. N.; Reed, C. A. *J. Am. Chem. Soc.* **1977**, *99*, 3641-3646.

(98) Mispelter, J.; Momenteau, M.; Lhoste, J. M. *Mol. Phys.* **1977**, *33*, 1715-1728.

(99) Wayland, B. B.; Mehne, L. F.; Swartz, J. J. *J. Am. Chem. Soc.* **1978**, *100*, 2379-2383.

(100) Migita, K.; La Mar, G. N. *J. Phys. Chem.* **1980**, *84*, 2953-2957.

(101) Latos-Grazynski, L.; Cheng, R.-J.; La Mar, G. N.; Balch, A. L. *J. Am. Chem. Soc.* **1982**, *104*, 5992-6000.

(102) The usual practice of reporting isotropic shifts instead of chemical shifts for paramagnetic NMR spectra¹⁰³ is abandoned in this paper because of the ambiguity that arises when attempting to assign completely the spectrum of Fe(OEC). For consistency, chemical shifts are also reported for Fe(OEP).

(103) Jesson, J. P. In "NMR of Paramagnetic Molecules"; La Mar, G. N., Horrocks, Jr., W. D., Holm, R. H., Eds.; Academic Press: New York, 1973; pp 1-52.

(104) Strauss, S. H.; Holm, R. H., unpublished results, 1980.

(105) For H₂(OEC) see ref 60 and references therein; for Zn(OEC) see Experimental Section.

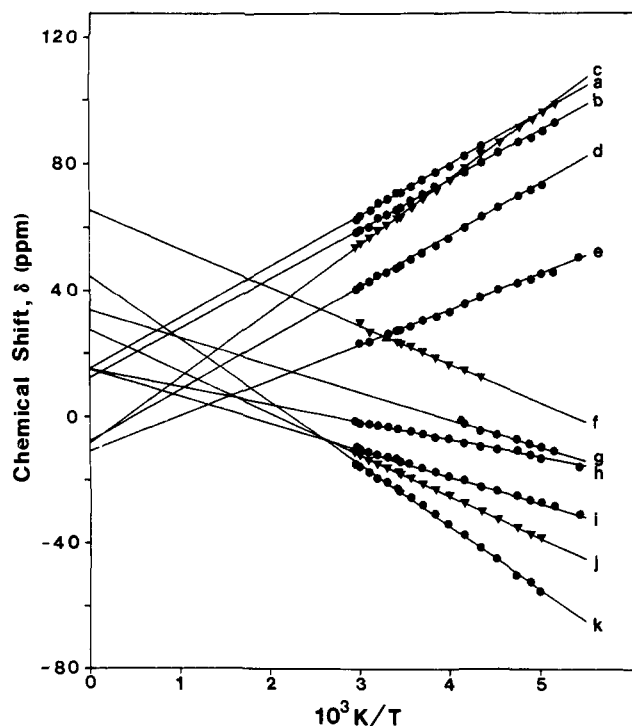


Figure 5. δ vs. $1/T$ plots for 200-MHz ^1H NMR spectra of Fe(OEC) in toluene- d_6 . The solid lines are linear least-squares fits to the data and are extrapolated to $1/T = 0$.

peratures. The linearity of δ vs. $1/T$ for each resonance demonstrates that the $S = 1$ ground state of Fe(OEC) is not in thermal equilibrium with other spin states, as was also shown for Fe(OEP) (see above) and for Fe(TPP).⁹⁷ The similarity ends there. Extrapolation of δ vs. $1/T$ plots to $1/T = 0$ does not yield the diamagnetic value (Zn(OEC) reference) for any of the protons of Fe(OEC). The pattern of upfield and downfield shifts strongly suggests that (i) protons on symmetry equivalent pyrrole rings (resonances c-e) experience isotropic shifts that move downfield with decreasing temperature and have $1/T = 0$ intercepts upfield of the diamagnetic value and (ii) protons on the unique pyrrole ring and on the pyrroline ring (resonances f-k) experience isotropic shifts that move upfield with decreasing temperature and have $1/T = 0$ intercepts downfield of the diamagnetic value (by as much as ~ 60 ppm). These observations are consonant with in-plane magnetic anisotropy and a resultant rhombic component to the dipolar shift (i.e., $\chi_{xx} \neq \chi_{yy}$).¹⁰³

$$(\Delta H/H)^{\text{dip}} = (-1/3N)[\chi_{zz} - 1/2(\chi_{xx} + \chi_{yy})]\{(3 \cos^2 \theta - 1)/r^3\} - (1/2N)[\chi_{xx} - \chi_{yy}]\{\sin^2 \theta \cos 2\phi/r^3\}$$

where N is Avogadro's number, χ_{xx} , χ_{yy} , and χ_{zz} are the magnetic susceptibilities along the three principal magnetic axes, and r , θ , and ϕ are the spherical polar coordinates of a proton with respect to the metal atom origin. Note that a negative $(\Delta H/H)^{\text{dip}}$ produces a positive chemical shift (δ scale) downfield of the diamagnetic value.

For simplicity we transfer the D_{4h} coordinate system of Fe(OEP) to Fe(OEC), treating the loss of 4-fold symmetry from the reduction of one pyrrole ring as a perturbation. Thus z is perpendicular to the plane of Fe(OEC) and y is coincident with the molecular C_2 axis. Within this framework we can begin to estimate the magnetic anisotropy of Fe(OEC). We note first that the δ vs. $1/T$ behavior of the meso protons of Fe(OEC) and Fe(OEP) is very similar (sign and magnitude of the slopes, and $1/T = 0$ intercepts close to the diamagnetic values). With this coordinate system, the rhombic component of $(\Delta H/H)^{\text{dip}}$ is zero for the meso protons of Fe(OEC) (since $\cos 2\phi = 0$ for $\phi = 45^\circ$, 135° , 225° , and 315°) while the axial component is a constant ($\theta = 90^\circ$ for both types of meso proton). Therefore the small difference in slopes for resonances a and b must derive from small

differences in contact shifts. Nevertheless, if the contact contributions to the isotropic shifts are similar for the meso protons of Fe(OEC) and Fe(OEP), then $[\chi_{zz} - 1/2(\chi_{xx} + \chi_{yy})]$ is also similar (and negative⁹⁷) for these two compounds.

The spin delocalization mechanism for $S = 1$ Fe(II) porphyrins has been shown to be $P \rightarrow Fe \pi$ charge transfer.^{97,98} Thus the contact contribution to the isotropic shifts should be very small for methyl protons in Fe(OEC) and Fe(OEP). If one assumes that r and θ are equal for all pyrrole methyl protons in these two compounds, the similarity in axial anisotropy suggested above allows the rhombic component of the dipolar shift of these methyl protons to be estimated.¹⁰⁶ The slope for resonance e in Figure 5 is larger than the slope for the methyl protons of Fe(OEP) by an amount equal to the rhombic component (note that this requires $\chi_{xx} > \chi_{yy}$). The slope for the methyl protons of the unique pyrrole ring of Fe(OEC) (either resonance h or i) should be the difference of the constant axial component (3.4×10^3 ppm·K) and the rhombic component (7.8×10^3 ppm·K). The agreement between the calculated slope, -4.4×10^3 ppm·K, and the slope of resonances h and i is striking, given the simplicity of our analysis. The rhombic component is roughly twice the magnitude of the axial component, and, for the reasonable values $\theta = 70^\circ$, $\phi = 0^\circ$, we calculate $[\chi_{xx} - \chi_{yy}] \approx [\chi_{zz} - 1/2(\chi_{xx} + \chi_{yy})]$. Clearly many approximations have been made in the foregoing analysis. Since Fe(OEC) possesses C_2 symmetry, the only magnetic axis that must coincide with the molecular framework is the C_2 axis. If we assume (i) that Fe(OEC) possesses axial anisotropy ($C_2 = z$), (ii) that the contact contributions to the isotropic shifts of the methyl proton resonances are small, (iii) that $\theta = 0^\circ$ or 180° for the methyl protons on the z axis and $\theta \approx 90^\circ$ for the methyl protons on the symmetry equivalent pyrrole rings, and (iv) that r is similar for all pyrrole methyl protons, then we calculate that the slope for resonance h or i should be opposite in sign and roughly twice the magnitude of the slope for resonance e. This expectation is not observed (Table XI). Therefore, even when a proper coordinate system in which z corresponds to the molecular C_2 axis is used, the only way to account for the slopes of resonances e, h, and i of Fe(OEC) is to conclude that $(\Delta H/H)^{\text{dip}}$ has sizable axial and rhombic components.

In ongoing work,¹⁰⁷ we are comparing the temperature dependence of ^1H NMR spectra of other Fe(II) porphyrins, chlorins, and isobacteriochlorins and are attempting to measure χ_{xx} , χ_{yy} , and χ_{zz} of deuterated samples of Fe(OEC) and Fe(OEP) by high-field ^2H NMR spectroscopy.^{108,109} These experiments will allow us to confirm our assignments and to separate the dipolar and contact portions of the isotropic shifts. A more complete analysis of the temperature dependence of the ^1H NMR spectra of Fe(OEC) and Fe(OEP) must await these results. Nevertheless, we feel that the evidence for significant in-plane magnetic anisotropy for Fe(OEC) is compelling.

At the present time, we cannot offer a conclusive interpretation for the unusual $1/T = 0$ intercepts observed for Fe(OEC) (Figure 5 and Table XI). Similar non-Curie behavior has been observed for low-spin Fe(III) porphyrins.¹¹⁰ For these $S = 1/2$ systems, two explanations have been offered: (i) the deviations result from a temperature-independent contact shift which itself results from a considerable temperature dependence of the hyperfine coupling constant A ;¹¹¹⁻¹¹³ (ii) the deviations result from a seemingly temperature-independent second-order Zeeman (SOZ) contribution to the dipolar shift.^{114,115} The latter explanation has been

(106) The values estimated for the time averages $\langle r \rangle$, $\langle \theta \rangle$, and $\langle \phi \rangle$ are noted here simply as r , θ , and ϕ .

(107) Strauss, S. H.; Pawlik, M. J.; Long, K. M., unpublished data, 1984.

(108) Domaille, P. J.; Harlow, R. L.; Ittel, S. D.; Peet, W. G. *Inorg. Chem.* **1983**, *22*, 3944-3952 and references therein.

(109) Lohman, J. A. B.; MacLean, C. *J. Magn. Reson.* **1981**, *42*, 5-13 and references therein.

(110) Walker, F. A.; Benson, M. *J. Phys. Chem.* **1982**, *86*, 3495-3499 and references therein.

(111) Wuthrich, K. *Struct. Bonding* **1953**, *8*, 53.

(112) von Goldammer, E.; Zorn, H. *Mol. Phys.* **1976**, *32*, 1423-1435.

(113) von Goldammer, E.; Zorn, H.; Daniels, A. *J. Magn. Reson.* **1976**, *23*, 199-210.

offered for this type of non-Curie behavior in other $S = 1/2$ ¹¹⁶ and $S \geq 1$ ^{117,118} systems. In some cases the SOZ contribution to $(\Delta H/H)^{\text{dip}}$ is believed to be larger than the first-order Zeeman contribution.^{114,115,117} A third explanation, (iii), is possible for $S \geq 1$ systems with a large zero-field splitting (ZFS).^{117,118} In these cases, $(\Delta H/H)^{\text{dip}}$ contains both $1/T$ and $1/T^2$ terms. In principle, this should lead to a nonlinear δ vs. $1/T$ plot. However, the experimental range of temperatures may be too small to detect the curvature. Thus, it is possible for proton resonances having sizable pseudocontact shifts to follow a $1/T$ dependence experimentally but to have a $1/T = 0$ intercept considerably different from the diamagnetic value.^{117,118}

We believe that explanation i is not likely to account for our observations because the $1/T = 0$ intercepts for the methyl protons of Fe(OEC) are very different from the corresponding diamagnetic values (see Table XI). As noted above, the contact contributions to the isotropic shifts should be very small for these protons.^{97,98} If explanation ii accounts for the observed intercepts, then $[\chi_{zz} - 1/2(\chi_{xx} + \chi_{yy})]$ for Fe(OEC) should have a negligible or minor SOZ component while $[\chi_{xx} - \chi_{yy}]$ should have a significant SOZ component. Explanation iii has only been treated theoretically for axial systems with one ZFS term, D .^{117,118} Note that Fe(OEP) has "normal" $1/T = 0$ intercepts, even though it probably has a large D , as does Fe(TPP) (Table XI). Two ZFS parameters, D and E , would be required to describe the rhombic anisotropy of Fe(OEC). Magnetic susceptibility measurements (solution and

solid state) are under way for this compound.

Conclusions

The four-coordinate square-planar molecular structures of Fe(OEC) and Fe(OEP) have been found to be similar. The "small" μ_{eff} and "large" quadrupole splitting of Fe(OEC), however, show that the electronic structures of the two compounds are significantly different despite their common $S = 1$ ground state. Variable-temperature ¹H NMR spectra show that Fe(OEC) possesses rhombic anisotropy. This is the first example of resolvable ring-induced rhombicity in a metallohydroporphyrin. Whether the differences we have discovered between iron porphyrins and hydroporphyrins are to be found for other oxidation states, spin states, and ligation states remains to be seen.

Acknowledgment. This work was supported by grants from the Research Corporation (to S.H.S.) and the National Institutes of Health (HL 13157 to J.A.I. and GM 31554 to S.H.S.) and by a CSU Biomedical Research Support Grant (537272 to S.H.S.). We thank Dr. E. J. Moore, M. J. Pawlik, and M. M. Miller for technical assistance. We also thank C. E. Bronnimann for recording some preliminary 360-MHz ¹H NMR spectra in the Colorado State University Regional NMR Center, which is funded by National Science Foundation Grant No. CHE-8208821.

Registry No. Fe(OEP), 61085-06-1; Fe(OEC), 78319-96-7.

Supplementary Material Available: Table III (anisotropic thermal parameters and hydrogen atom positions for Fe(OEP)), Table IV (anisotropic thermal parameters and hydrogen atom positions for Fe(OEC)), Table V (least-squares planes for Fe(OEP)), Table VI (least-squares planes for Fe(OEC)), Table VII (structure amplitudes for Fe(OEP)), and Table VIII (structure amplitudes for Fe(OEC)) (30 pages). Ordering information can be found on any current masthead page.

(114) Horrocks, Jr., W. D.; Greenberg, E. S. *Biochim. Biophys. Acta* **1973**, *322*, 38-44.

(115) Horrocks, Jr., W. D.; Greenberg, E. S. *Mol. Phys.* **1974**, *27*, 993-999.

(116) McGarvey, B. R. *J. Chem. Phys.* **1970**, *53*, 86-91.

(117) Kurland, R. J.; McGarvey, B. R. *J. Magn. Reson.* **1970**, *2*, 286-301.

(118) McGarvey, B. R. *J. Am. Chem. Soc.* **1972**, *94*, 1103-1108.

Vanadium(V) Oxyanions: The Esterification of Ethanol with Vanadate

Michael J. Gresser and Aln S. Tracey*

Contribution from the Department of Chemistry, Simon Fraser University, Burnaby, B.C., Canada V5A 1S6. Received January 15, 1985

Abstract: Vanadium-51 nuclear magnetic resonance (NMR) spectroscopy has been used to study the interaction of vanadate, V_i , with ethanol in aqueous solution. At the concentrations employed in this study vanadate existed in water as a monomeric tetrahedral species giving rise to a single resonance in the NMR spectrum. Upon partial replacement of water with ethanol two additional signals appeared. The response of these three resonances to changes in ethanol concentration and pH was consistent with their origin in inorganic vanadate and the esters ethyl vanadate and diethyl vanadate. From the variation in ethanol concentration, the following equilibrium constants were determined: $K_1 = [\text{EtOVO}_3\text{H}^-][\text{H}_2\text{O}]/[\text{EtOH}][\text{VO}_4\text{H}_2^-] = 10.4$ and $K_2 = [(\text{EtO})_2\text{VO}_2^-][\text{H}_2\text{O}]/[\text{EtOH}][\text{EtOVO}_3\text{H}^-] = 2.3$. From the effect of pH on the chemical shifts and the concentration ratio of V_i to ethyl vanadate, the $\text{p}K_a$'s vanadate and ethyl vanadate were determined to be 8.3 and 8.9, respectively. Variable-temperature NMR studies of a solution prepared at pH 7.5 and containing 3.4 M ethanol and 7.8×10^{-5} M V_i showed coalescence of the vanadate and ethyl vanadate resonances at 328 K. From this and the equilibrium constant, a value of $1.2 \times 10^3 \text{ s}^{-1}$ for the pseudo-first-order rate constant of ethyl vanadate hydrolysis at this pH and temperature was determined.

Vanadium is a widely dispersed element which, as an essential nutrient, has its major effect on the action of enzymes.^{1,2} The element is important for most biological systems when in the vanadium(IV) and vanadium(V) oxidation states. It has recently

been found that vanadium(V) oxyanions (V_i) strongly activate the glucose dehydrogenase activity of glucose 6-phosphate dehydrogenase and that this activation can be rationalized in terms of the rapid nonenzymic formation of glucose 6-vanadate.³ In

(1) Chasteen, N. D. *Struct. Bonding* **1983**, *53*, 105-138.

(2) Ramasarma, T.; Crane, F. L. *Curr. Top. Cell. Reg.* **1981**, *20*, 247-301.

(3) Nour-Eldeen, A. F.; Craig, M. M.; Gresser, M. J. *J. Biol. Chem.* in press.